Hybrid plasmon waveguides with metamaterial substrate and dielectric substrate: A contrastive study*

Gong Hui(宫 慧), Liu Yu-Min(刘玉敏)†, Yu Zhong-Yuan(俞重远), Wu Xiu(吴 秀), and Yin Hao-Zhi(尹昊智)

State Key Laboratory of Information Photonics and Optical Communications, Beijing University of Posts and Telecommunications, Beijing 100876, *China*

(Received 16 June 2013; revised manuscript received 23 August 2013; published online 10 February 2014)

Hybrid plasmon waveguides, respectively, with metamaterial substrate and dielectric substrate are investigated and analyzed contrastively with a numerical finite element method. Basic properties, including propagation length L_p, effective mode area A_{eff}, and energy distribution, are obtained and compared with waveguide geometric parameters at 1.55 μm. For the waveguide with metamaterial substrate, propagation length L_p increases to several tens of microns and effective mode area A_{eff} is reduced by more than 3 times. Moreover, the near field region is expanded, leading to potential applications in nanophotonics. Therefore, it could be very helpful for improving the integration density in optical chips and developing functional components on a nanometer scale for all optical integrated circuits.

Keywords: hybrid plasmon waveguide, metamaterial, propagation length, effective mode area

PACS: 61.46.Km, 78.67.Pt **DOI:** 10.1088/1674-1056/23/4/046103

1. Introduction

As one of the most rapidly growing areas of research, the surface plasmon polariton (SPP) waveguide has attracted much attention due to its promising applications in a wide spectral region and capability of manipulating electromagnetic field on a subwavelength scale. Although the above advantages can be utilized to reduce the chip area and improve integration,[1–3] the SPP waveguide still faces significant challenges in the trade-off between propagation loss and field confinement, which means that strong field confinement usually leads to a high propagation loss. In this circumstance, Oulton *et al.*[4] reported on a hybrid plasmon waveguide capable of subwavelength confinement in two dimensions with a low propagation loss. Since then, various types of hybrid SPP waveguides have been proposed and the nanowire-substrate waveguide has become an important part of them.[5–10] In practical applications, appropriate substrate is of great importance for waveguide performance. For this reason, Wang *et al.*[11] investigated the plasmon modes of Ag nanowire coupled with different dielectric substrates, including magnesium fluoride (MgF_2), silica (SiO_2), indium tin oxide (ITO), and titanium dioxide (TiO_2).[11] Zhang and Xu[12] optimized the substrate-mediated plasmon coupling toward high-performance plasmon nanowire waveguides by adding a high-permittivity layer onto the low-permittivity substrate. However, more complex multilayer substrate has not been adequately investigated to modify the waveguide performance.

Recently, He *et al.*[13] proposed nanoscale slot waveguides of multilayer metamaterial for achieving large optical field enhancement, indicating that the predicted giant optical forces are achievable in experiment. Created from extremely thin, alternating layers of metal and dielectric, metamaterial structures can provide unique optical properties and be useful for a number of advanced applications and devices.[14–16] Inspired by the finer performances of metamaterial, we propose a new type of hybrid plasmon waveguide with metamaterial substrate and calculate its several performance parameters. For comparison, a waveguide with traditional dielectric substrate is also considered. The results show that by adopting metamaterial substrate, we can achieve lower propagation loss, longer propagation length, smaller effective mode area, and stronger field enhancement simultaneously.

The rest of this paper is organized as follows. In Section 2 the waveguide structures of two hybrid plasmon waveguides are outlined. In Section 3 the contrastive results of the two waveguides by applying a numerical finite element method are presented. Finally, some conclusions are drawn from the present studies in Section 4.

2. Waveguide structure

The schematics of the two hybrid plasmon waveguides are shown in Fig. 1. The radius of Ag nanowire is R and the gap width is t. For an optical communication wavelength of 1.55 μm, the relative permittivity of silver and silica are $\varepsilon_{Ag} = -129 + 3.3i$ and $\varepsilon_{SiO_2} = 2.1$, respectively. Since both structures are placed in air and all materials are considered as being non-magnetic in our research, the relative permeability of all materials is set as $\mu_r = 1$.[17]

*Project supported by the National Natural Science Foundation of China (Grant Nos. 60908028, 60971068, 10979065, and 61275201) and the Program for the New Century Excellent Talents in University, China (Grant No. NCET-10-0261).

†Corresponding author. E-mail: microliuyumin@hotmail.com

© 2014 Chinese Physical Society and IOP Publishing Ltd

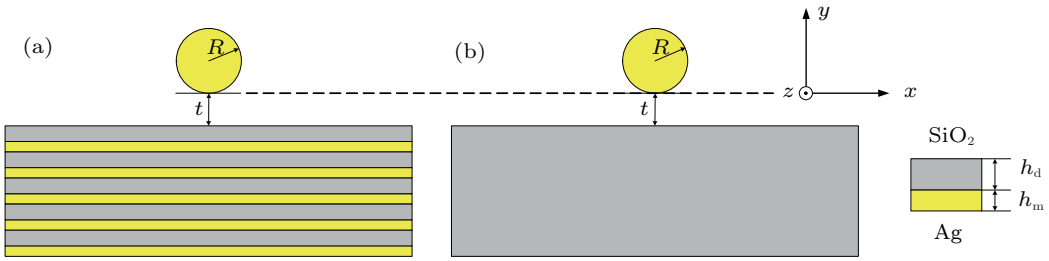


Fig. 1. (color online) Schematics of hybrid plasmon waveguides with metamaterial substrate (a) and dielectric substrate (b). Both structures are placed in air.

For the first model, the heights of metal and dielectric components of metamaterial substrate are set to be h_{m} and h_{d}, respectively. Based on effective medium theory (EMT), the metamaterial structure can be considered as a homogeneous effective medium and the principle components of the relative permittivity tensor are determined as follows:[18]

$$\varepsilon_x = \varepsilon_z = f_{\mathrm{m}}\varepsilon_{\mathrm{m}} + (1 - f_{\mathrm{m}})\,\varepsilon_{\mathrm{d}}, \tag{1}$$

$$\varepsilon_y = \varepsilon_{\mathrm{m}}\varepsilon_{\mathrm{d}}/[f_{\mathrm{m}}\varepsilon_{\mathrm{d}} + (1 - f_{\mathrm{m}})\,\varepsilon_{\mathrm{m}}], \tag{2}$$

where f_{m} is the volume filling ratio of metal, ε_{m} and ε_{d} are the relative permittivity values of metal and dielectric medium, respectively. For instance, $\varepsilon_x = \varepsilon_z = -50.34 + 1.32\mathrm{i}$, $\varepsilon_y = 3.5384 + 0.001\mathrm{i}$ at $f_{\mathrm{m}} = 0.4$, which are quite different from the relative permittivity tensor of silica. To ensure simulation accuracy and reduce calculation complexity, we choose $f_{\mathrm{m}} = 0.4$, $h_{\mathrm{m}} = 4$ nm, and $h_{\mathrm{d}} = 6$ nm,[13,19] and truncate the computation domain by the perfectly matched layers (PMLs) with a thickness of half a wavelength in vacuum. Aiming at operating the hybrid plasmon waveguides with tight confinement, we study only the lowest order mode as it plays a central role and dominates the propagation properties.[20]

The propagation constant β, and propagation length L_{p} are defined as[21]

$$\beta = \mathrm{Re}(\beta) + \mathrm{iIm}(\beta), \tag{3}$$

$$L_{\mathrm{p}} = 1/[2\mathrm{Im}(\beta)]. \tag{4}$$

The propagation loss α is inversely proportional to L_{p} and expressed as

$$\alpha = 10\log(\mathrm{e})/L_{\mathrm{p}} \approx 4.343/L_{\mathrm{p}}. \tag{5}$$

To quantify local field enhancement, the effective mode area A_{eff} is defined as the radio of a mode total energy density per unit length and its peak energy density, i.e.,

$$A_{\mathrm{eff}} = W/\max\{W(r)\} = \iint_{\mathrm{all}} W(r)\,\mathrm{d}A/\max\{W(r)\}, \tag{6}$$

where $W(r)$ is the energy density and expressed as

$$W(r) = \frac{1}{2}\left(|E(r)|^2\,\mathrm{d}(\varepsilon(r)\omega)/\mathrm{d}\omega + \mu_0|H(r)|^2\right), \tag{7}$$

where $|E(r)|^2$ and $|H(r)|^2$ are the electric and magnetic fields, $\varepsilon(r)$ is the electric permittivity, and μ_0 is the vacuum magnetic permeability.[22]

3. Results and discussion

Based on the models in Section 2, we investigate and analyze the property parameters of the two hybrid plasmon waveguides in this section. A finite element method (FEM) is used to perform the following numerical calculations.

3.1. Mode profiles

As the magnetic field energy is much smaller than electric field energy, we use electric field energy distribution as the metric of whole electromagnetic energy distribution in the present work. Under this circumstance, the mode profiles in terms of electric field amplitude for waveguides with different substrates and gaps are shown in Fig. 2.

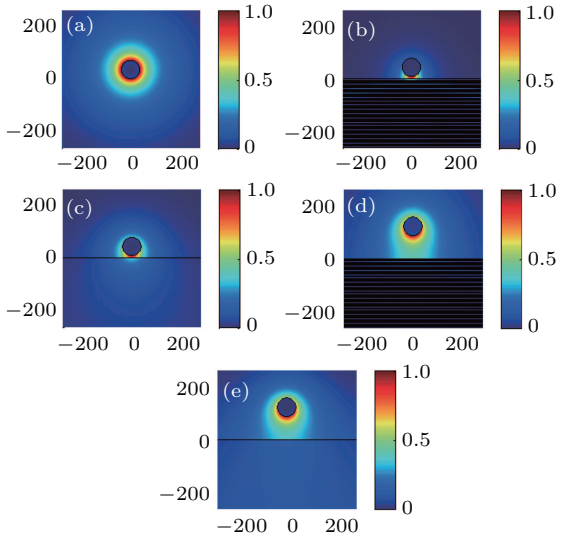


Fig. 2. (color online) Mode profiles in terms of electric field amplitude in the cases: (a) no substrate, free-standing in air, (b) metamaterial substrate, $t = 10$ nm, (c) dielectric substrate, $t = 10$ nm, (d) metamaterial substrate, $t = 100$ nm, and (e) dielectric substrate, $t = 100$ nm. The radius of nanowire is 40 nm.

As the abrupt changes of ε_y on air-nanowire and substrate-air interfaces, it is revealed that the enhancement of electric field appears in the gap region for all the waveguides above. While the free-standing waveguide reveals a symmetric mode profile (Fig. 2(a)), other hybrid plasmon waveguides

break the symmetry and confine electric field energy in gap region due to the existence of substrate (Figs. 2(b)–2(e)). With the increase of gap t, the confinement capacity of hybrid plasmon waveguide decreases, leading to the following results: (i) electric energy focuses on the surface of nanowire instead of in the region between nanowire and substrate; (ii) the magnitude of electric energy decreases.

In order to obtain a more obvious comparison, the normalized electric field amplitudes along the y direction are shown in Fig. 3 and the relative values at point of origin are displayed in Table 1.

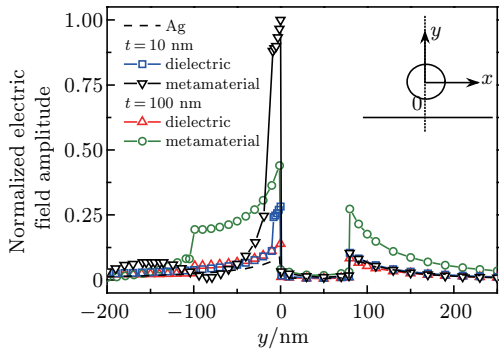


Fig. 3. (color online) Normalized electric field amplitudes along the y direction. The radius of R is 40 nm.

When the gap t varies from 10 nm to 100 nm, the electric field amplitudes have more than half the electric field amplitudes for waveguides with metamaterial and dielectric substrates, resulting from the reduced field confinement capability. On the other hand, at an identical gap t, the electric field amplitude for waveguide with metamaterial substrate can be more than 3 times stronger than that for waveguide with dielectric substrate, owing to tight optical mode confinement enabled by the ultrahigh refractive indices supported by metamaterial.

Table 1. Relative values of electric field amplitudes at the origin point.

Substrate types	$t = 10$ nm	$t = 100$ nm
Metamaterial	1	0.44
Dielectric	0.28	0.13

3.2. Waveguiding properties relative to radius R

In order to further study the hybrid plasmon waveguides, we investigate the dependences of basic properties, including propagation length L_p, effective mode area A_{eff}, and energy distribution on waveguide geometric parameters at 1.55 μm.

For the waveguide with metamaterial substrate, the propagation length L_p changes from a few micrometers to several tens of microns (lines with solid symbols in Fig. 4(a)). For a quantitative comparison, part of the calculated data of L_p are listed in Table 2.

Within the range of calculation, we can classify the curves of L_p into three types: normal gentle type, consistently

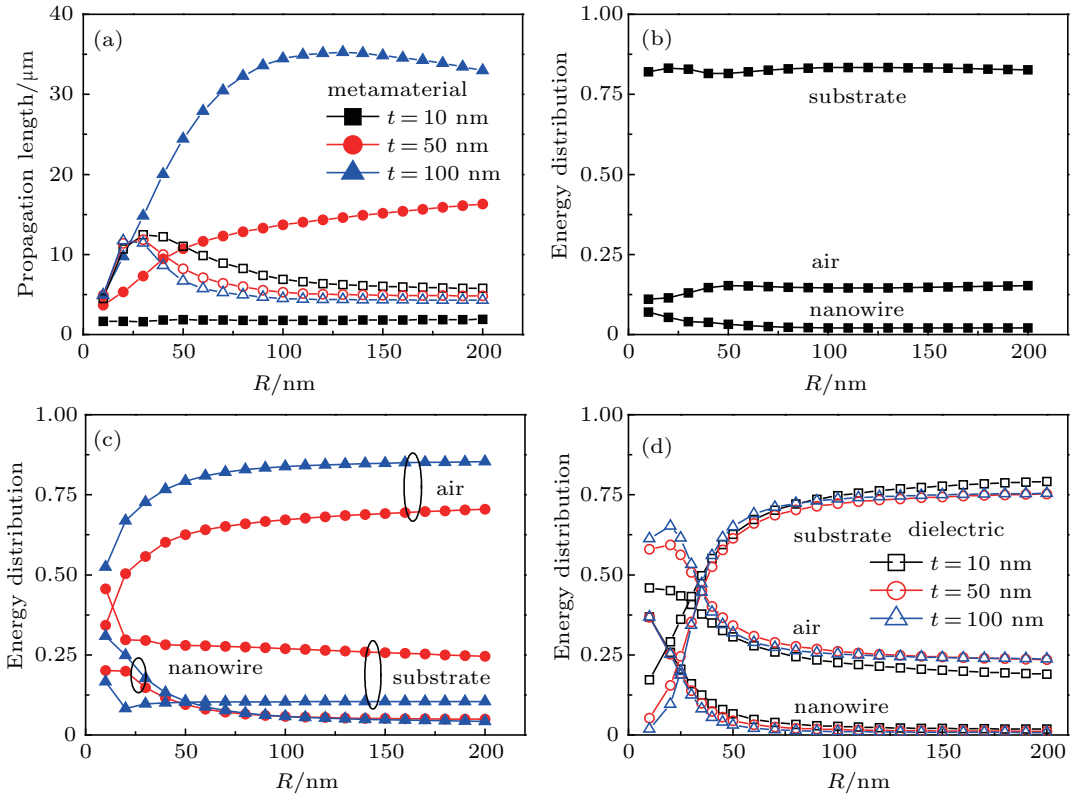


Fig. 4. (color online) Plots of (a) values of propagation length L_p and ((b)–(d)) energy distributions for waveguides with metamaterial and dielectric substrates versus radius R for three different values of gaps t.

Table 2. Values of propagation length L_p versus radius R for waveguide with metamaterial substrate for three different values of gap t.

L_p/μm	$R = 20$/nm	$R = 50$/nm	$R = 100$/nm	$R = 150$/nm	$R = 200$/nm
$t = 10$/nm	1.66	1.84	1.77	1.81	1.89
$t = 50$/nm	5.33	10.74	13.70	15.15	16.32
$t = 100$/nm	9.76	24.42	34.45	34.84	32.98

increasing type, and first-increasing- then-decreasing type. When $t = 10$ nm, L_p is restricted to a few micrometers, presenting high and stable propagation loss. This occurs because more than three-quarter electromagnetic energy is confined in metamaterial substrate as the existence of a silver component, causes the energy in air gap to be unable to support long distance transport of light, which is shown in Fig. 4(b). When $t = 50$ nm, L_p continues to grow and tends towards stability until L_p reaches 20 μm. When $t = 100$ nm, although L_p first increases and then decreases, it is over 20 μm within a long range of R and its maximum exceeds 35 μm. The corresponding energy distributions for $t = 50$ nm and 100 nm are shown in Fig. 4(c), where most of energy is stored in the air region with the increase of radius R. In short, for a waveguide with metamaterial substrate, the propagation length L_p has a high sensitivity to gap t.

For the waveguide with dielectric substrate, it is interesting to notice that the three curves of propagation length L_p (lines with hollow symbols in Fig. 4(a)) first rise and then fall with similar values for different values of gap t. Also, their maxima appear at $R = 25$ nm almost simultaneously. As an illustration, we show the energy distributions of the waveguide with dielectric substrate in Fig. 4(d) for different values of gap t. When $R < 25$ nm, the energy existing in air is dominant and the proportion of energy in substrate is less than fifty percent, resulting in an increased propagation length. However, the scenario is reversed when $R > 25$ nm. With the increase of R, increasing energy concentrates in dielectric substrate and is gradually stabilizing. Furthermore, there are only slight differences among the energy distribution curves with different values of gap t, meaning that the propagation length L_p has a low sensitivity to gap t.

To further explore the properties of the above hybrid plasmon waveguides, the curves of effective mode area are shown in Fig. 5.

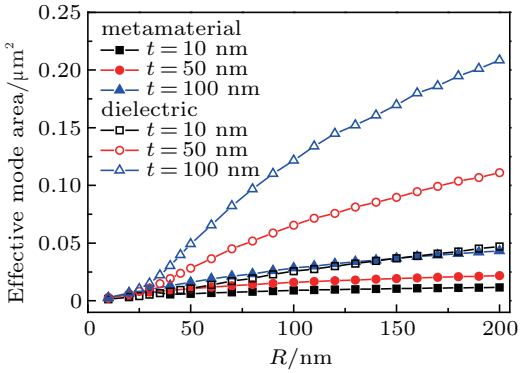


Fig. 5. (color online) Plots of effective mode area A_{eff} versus radius R for waveguides with metamaterial and dielectric substrates.

In general, all the curves increase monotonically with the increase of radius R and gap t, and their values are very close to each other when $R < 30$ nm. However, different lines have their own growth rates. For the waveguide with metamaterial substrate, the slopes of symbol lines versus radius are much smaller, representing that the A_{eff} increases more slowly and its values are reduced by 3∼5 times within a wide region of R (Table 3).

Table 3. Ratios of A_{eff} versus radius R for dielectric substrate and metamaterial substrate.

Dielectric/Metamaterial	$R = 30$/nm	$R = 50$/nm	$R = 100$/nm	$R = 150$/nm	$R = 200$/nm
$t = 10$/nm	1.23	1.77	2.87	3.48	4.09
$t = 50$/nm	1.46	2.69	4.12	4.66	5.11
$t = 100$/nm	1.54	3.08	4.29	4.61	4.82

3.3. Waveguiding properties relative to gap *t*

The plots of propagation length L_p, effective mode area A_{eff}, and energy distribution versus gap t for waveguides with metamaterial and dielectric substrates are shown in Fig. 6. For the waveguide with metamaterial substrate, within the range of our research, L_p reveals a progressive trend when $R = 40$ nm and 70 nm while it first increases and then decreases when $R = 100$ nm (Fig. 6(a)). However, we can predict that a similar decrease will appear as t continues to grow for the cases of $R = 40$ nm and 70 nm. Based on Ref. [23], when a silver nanowire moves away from the silica substrate, the L_p first increases, then quickly falls. After that, it slowly increases again. Therefore, the gap width can be divided into three regions: the near field, dissipation field, and far field regimes, respectively, which correspond to different loss mechanisms and propagation lengths.[23] In our work, due to the existence

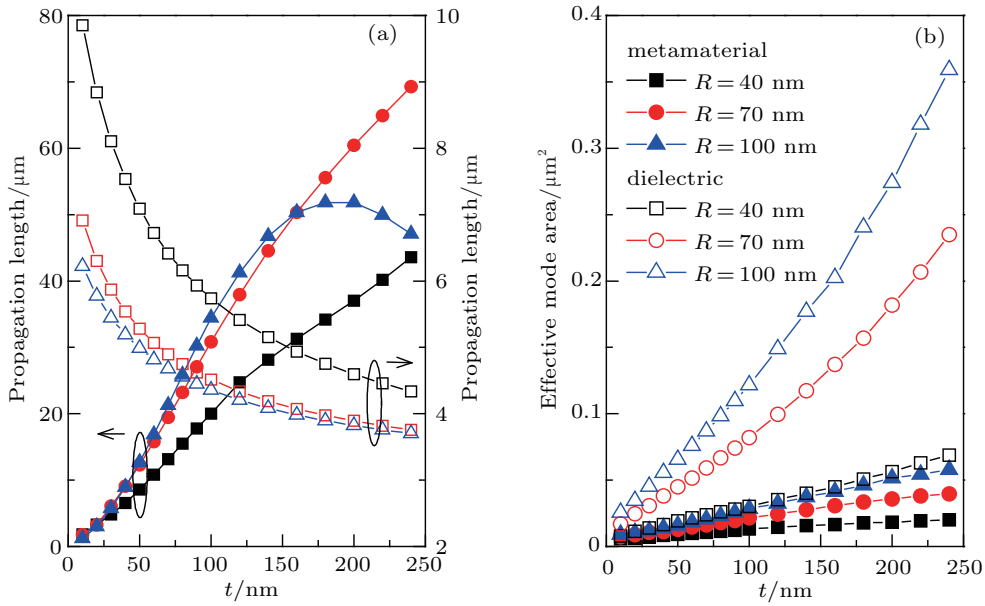


Fig. 6. (color online) Plots of (a) propagation length L_p and (b) effective mode area A_{eff} versus gap t for waveguides with metamaterial and dielectric substrates.

of metamaterial substrate, the boundaries of three regions are changed and the scope of near field region is much expanded, leading to several tens of micro long propagation length in our range of interest. For the waveguide with dielectric substrate, the L_p decreases monotonically under all the values of radius R and exhibits the dissipation field region only (Fig. 6(a)).

As for effective mode areas (Fig. 6(b)), we can reconfirm that they monotonically increase as gap t and radius R increase, and have similar conclusions to those in Fig. 5. That is, for the waveguide with metamaterial substrate, the values of A_{eff} are reduced by several times with the increase of gap t. Table 4 shows the ratios of A_{eff} for dielectric substrate and metamaterial substrate versus gap t under different radii. With the increase of t, the value of ratio increases as well. Furthermore, the larger the radius R, the more obvious the increase becomes.

Table 4. Ratios of A_{eff} versus gap t for dielectric substrate and metamaterial substrate.

Dielectric /Metamaterial	$t = 10$/nm	$t = 60$/nm	$t = 120$/nm	$t = 180$/nm	$t = 240$/nm
$R = 40$/nm	1.36	2.20	2.45	2.87	3.43
$R = 70$/nm	2.31	3.51	4.09	4.66	5.92
$R = 100$/nm	2.81	4.14	4.56	5.20	6.19

Energy distributions versus gap t for waveguides with metamaterial and dielectric substrates (Fig. 7) partly exhibit the above phenomena.

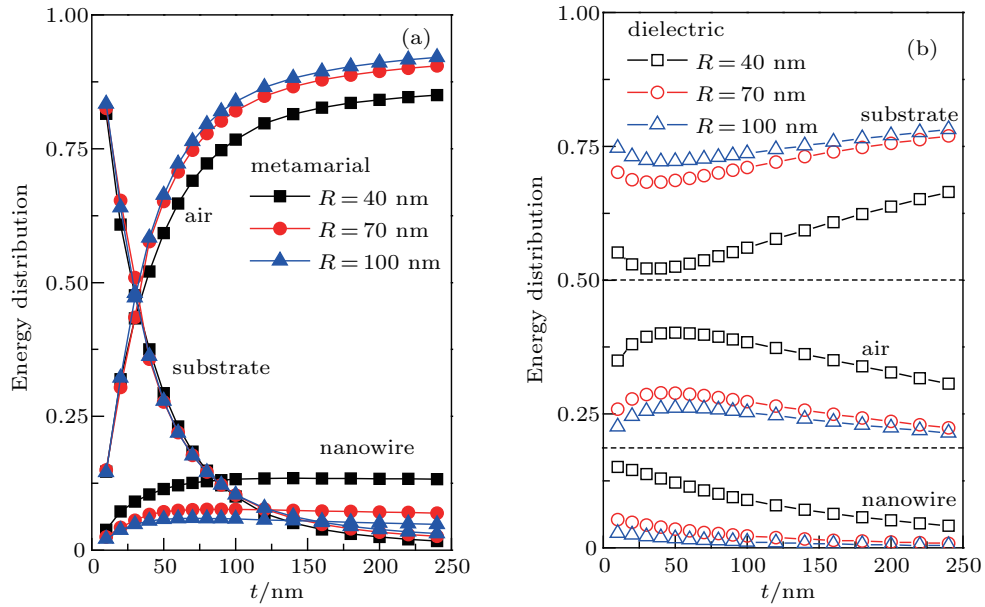


Fig. 7. (color online) Energy distributions versus gap t for waveguides with (a) metamaterial and (b) dielectric substrates.

For the waveguide with metamaterial substrate, the energy in air region increases with the increase of gap t and plays a growing dominant role, and the energy in nanowire first increases and then keeps unchanged, while the energy in substrate decreases all the time. For the waveguide with dielectric substrate, the energy in substrate decreases in beginning and then increases, which is the dominant driver and exceeds fifty percent in the whole range of interested gap t, the energy in air region is contrary to it, while the energy in nanowire reduces in the scope of our interest. In conclusion, the interactions between the light and metamaterial nanostructures generate unique effects on propagation length and effective mode area in our models, which will have great potential applications in nanophotonics field.

4. Conclusion

In this paper, we investigated and analyzed the hybrid plasmon waveguides, respectively, with metamaterial substrate and dielectric substrate, by using a numerical finite element method. The dependences of basic properties, including propagation length L_{p}, effective mode area A_{eff}, and energy distribution, on waveguide geometric parameters at 1.55 μm were obtained and compared. For the waveguide with metamaterial substrate, the propagation loss decreases and the propagation length increases from several to several tens of microns, the effective mode area is reduced by more than 3 times and the scope of near field region is expanded, leading to potential applications in nanophotonics. Therefore, our findings could be very helpful for improving the integration density in optical chips and developing the functional components on a nanometer scale for all optical integrated circuits.

References

[1] Barnes W L, Dereux A and Ebbesen T W 2003 *Nature* **424** 824
[2] Maier S A 2006 *IEEE J. Selected Topics Quantum Electron.* **12** 1671
[3] Liu J T, Xu B Z, Zhang J, Cai L K and Song G F 2012 *Chin. Phys. B* **21** 107303
[4] Oulton R F, Sorger V J, Genov D A, Pile D F P and Zhang X 2008 *Nat. Photon.* **2** 496
[5] Pfeiffer C A, Economou E N and Ngai K L 1974 *Phys. Rev. B* **10** 3038
[6] Khosravi H, Tilley D and Loudon R 1991 *J. Opt. Soc. Am. A* **8** 112
[7] Dong C H, Ren X F, Yang R, Duan J Y, Guan J G, Guo G C and Guo G P 2009 *Appl. Phys. Lett.* **95** 221109
[8] Shegai T, Huang Y, Xu H and Kall M 2010 *Appl. Phys. Lett.* **96** 103114
[9] Yan R, Pausauskie P, Huang J and Yang P 2009 *Proc. Natl. Acad. Sci.* **106** 21045
[10] Zhang L and Yang S 2013 *Chin. Phys. Lett.* **30** 034208
[11] Wang Y, Ma Y, Guo X and Tong L 2012 *Opt. Express* **20** 19006
[12] Zhang S and Xu H 2012 *ACS Nano* **6** 8128
[13] He Y, He S and Yang X 2012 *Opt. Lett.* **37** 2907
[14] Salandrino A and Engheta N 2006 *Phys. Rev. B* **74** 075103
[15] Jacob Z, Alekseyev L V and Narimanov E 2006 *Opt. Express* **14** 8247
[16] Narimanov E, Noginov M, Li H and Barnakov Y 2010 *Proceedings of Quantum Electronics and Laser Science Conference*, May 16–21, 2010, San Jose, USA
[17] Johnson P B and Christy R W 1972 *Phys. Rev. B* **6** 4370
[18] Foss C A Jr, Hornyak G L, Stockert J A and Martin C R 1994 *J. Phys. Chem.* **98** 2963
[19] He Y, He S, Gao J and Yang X 2012 *Opt. Express* **20** 22372
[20] Takahara J, Yamagishi S, Taki H, Morimoto A and Kobayashi T 1997 *Opt. Lett.* **22** 475
[21] Maier S A 2007 *Plasmonics: Fundamentals and Applications* (New York: Springer) pp: 53–62
[22] Oulton R, Bartal G, Pile D and Zhang X 2008 *New J. Phys.* **10** 105018
[23] Zou C L, Sun F W, Xiao Y F, Dong C H, Chen X D, Cui J M, Gong Q, Han Z F and Guo G C 2010 *Appl. Phys. Lett.* **97** 183102